

# Novel Magnetic Sensor Based on Fiber Bragg Grating and Magnetic Shape Memory Alloys

Carmen Ambrosino\*, Patrizio Capoluongo, Stefania Campopiano, Antonello Cutolo, Andrea Cusano  
Optoelectronic Division, Engineering Department, University of Sannio, Benevento, Italy

\* [carmen.ambrosino@unisannio.it](mailto:carmen.ambrosino@unisannio.it)

Michele Giordano

Institute for Composite and Biomedical Materials, National Research Council, Naples, Italy

Daniele Davino, Ciro Visone

Engineering Department, University of Sannio, Benevento, Italy

## ABSTRACT

In this work, the experimental demonstration of fiber Bragg grating (FBG) based sensors as magnetic transducers is reported. Up to now, FBGs based magnetic sensors have been proposed by using Terfenol, metallic alloy with a giant magnetostriction coefficient. Here, a novel configuration is proposed employing a new class of magnetic materials, Magnetic Shape Memory alloys (MSMs), instead of Terfenol. This class of material, with a very giant magnetostriction coefficient, changes its shape when magnetic fields are applied. High strain values, up to 10 percent can be obtained with fast response times (less than 1 ms). A FBG has been bonded on a MSM sample and sensor characterization has been carried out. Experimental results and comparison with Terfenol based FBGs sensors performances are reported, showing, for MSM, a sensitivity expressed as  $(\Delta\lambda_B/\lambda_B)/(\Delta H/H_m)$  of  $1.6e-4$ , where  $\lambda_B$  is Bragg wavelength and  $H_m$  the mean magnetic field in a considered range.

**Keywords:** fiber optic sensors, Fiber Bragg Gratings, magnetostriction, magnetic shape memory alloy MSM, Terfenol, magnetic field sensors.

## 1. Introduction

Magnetic/electric sensors have assisted mankind in analyzing and controlling thousands of function for many decades. There are many ways to sense magnetic fields, most of them based on the intimate connection between magnetic and electric phenomena and each magnetic sensing technique bases itself on physical phenomena, as Electromagnetic Induction (search coils) or superconductivity (SQUID) or on specific effects as Hall effect, magnetoresistance, Faraday polarization effect (magneto-optical sensors), Faraday effect, [1]. In last years a great number of applications of magnetic sensors, spreading from electrical power industry (power generators up to 1000MVA with voltages between 6 and 30 kV [2], direct currents sensor (up to 500 kA [3]) to control engineering (active control of structural vibrations in high precision machine-tools), robotics, and, in precision actuators in biomedical, aerospace and automotive fields, have gained great interest.

Such a wide set of applications can be grouped into three categories as showed in Table 1 in [1]: low-sensitivity applications (non contact switching), for fields larger than 1G; medium sensitivity (magnetic anomaly detection) and high sensitivity applications

(brain function mapping), the latter for fields lower than  $1e-5$  G.

For all these applications optical current sensors and in particular, fiber optic sensors (FOS) technology are a winning choice. In fact, it has been recognized that optical current sensors have many advantages compared to conventional iron-core current transformers, including their immunity to electromagnetic interference, high dynamic range, bandwidth, compact design, especially reduced complexity, and cost of insulation construction. [4]. Optic fibers can be integrated within host structures with a minimum alteration of its features thanks to their small dimensions and they can monitor locations inaccessible for other sensors (e.g. strain gages) [5, 6]. Moreover simultaneous multi-parameter measures can be performed by these devices, able to work in very harsh conditions [7, 8]. In particular, among optics devices, fiber Bragg gratings (FBGs) exhibit good features in terms of high sensitivity, resolution and bandwidth [8]. Competitive costs, high multiplexing capability and good structural robustness are typical advantages of this class of devices, too. Fiber Bragg Gratings (FBGs) transduce applied strain in wavelength shift, which is an absolute parameter, immune to power drifts along the measurement chain.

A critical aspect of FBGs-based sensors is the adequate detection of wavelength shifts. However, techniques based on passive optical filtering represent a good trade-off in terms of resolution, flexibility and costs [9].

Moreover FBGs, thanks to their high immunity to Electromagnetic interferences, low intrusivity and non-conducting behavior, naturally allow the realization of multi-point magnetic field sensors, also in those cases where strict safety conditions are required (i.e., in presence of high current). In general, the common mechanism used to detect magnetic field with FBG sensors is Faraday effect, which showed very low sensitivity. Therefore, different transducers have been employed. Recently, a magnetic field and current single-point sensor, has been proposed in [10], where encouraging characteristics in terms of sensitivity has been showed. Such device exploits the FBG bonded on a Terfenol-D magnetostrictive rod; which is strongly affected by magnetic fields. As a drawback, the Terfenol-D sensitivity strongly decreases as magnetic field approaches few tens of kA/m.

Along this line of argument, in this work, a novel FBG sensor configuration is proposed employing a new class of magnetic materials, Magnetic Shape Memory alloys (MSMs) able to work with magnetic field up to 400-500 kA/m. In particular, after a suitable bonding protocol choice, followed to improve sensor performances, a fiber Bragg grating has been bonded on a MSM sample and the magnetic field sensor characterization has been carried out.

Magnetic fields with different amplitudes have been applied to the structure and related FBG responses have been acquired. For the demodulation of these signals, a technique based on the use of a broadband light source and an in fiber grating optical filter, able to convert wavelength shifts in amplitude modulation, has been used [11]. The reversibility of magnetic-field-induced strain of MSM material has been obtained by a pre-stress of the material. Several tests have been performed in order to characterize the sensing system with different level of pre-stress, as will be shown in the following. Moreover, performances of such new device, are compared to those employing ordinary magnetostrictive Terfenol-D materials.

## 2. Methodology

### 2.1 Fiber Bragg gratings interrogation technique.

The interrogation system used for the proposed magnetic sensor relies on a low cost ratiometric technique based on optical filtering combined with broadband interrogation [11]. Using a chirped and strongly apodized FBG, an optic filter with a linear wavelength response can be obtained. The block diagram of the interrogation system is reported in Fig.1.

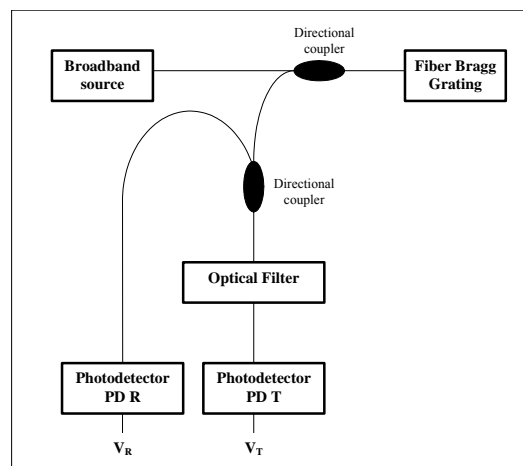


**Fig. 1** Interrogation sensor system-block diagram

The electronic processing of the two detected signals is performed according to, [2]:

$$V_n = \frac{V_T - K \cdot V_R}{V_T + K \cdot V_R} \quad (1)$$

where  $V_T$  is the transmitted voltage signal of PDT,  $V_R$  is the reflected voltage signal of PDR and  $K$  is a suitable constant.

The generated normalized signal,  $V_n$ , is a good measure of the “centre of mass” of the sensing grating spectrum, and, as a consequence, also of Bragg’s wavelength. Due to the passive nature of the proposed technique, system bandwidth is only limited by the electronic circuitry involved in the receiving unit. Static and dynamic resolutions of 1 pm and  $40\text{ne}/(\text{Hz})^{0.5}$  can be achieved up to 50 KHz.

### 2.2 Magnetic shape memory alloys (MSMs) working principle

Magnetically controlled shape memory (MSM) materials (Ni-Mn-Ga or Fe-Pd alloys), with a very large magnetoelastic coupling coefficient, are a new way to produce motion and force. MSM material consists of internal areas, twin variants. These variants have different magnetic and crystallographic orientations. When the actuating element made of MSM material is subjected to a magnetic field the proportions of the variants change resulting in the shape change of the element

Applying the magnetic field  $H$  to the single variant material causes the other twin variants to appear and grow. When magnetic field strength increases the boundaries between twins move, as amount of preferentially oriented twin variants grow at the expense of the other twin variants. Unit cells of the martensite phase in which MSM effect occurs in Ni-Mn-Ga alloys are tetragonal [13].

Magnetic anisotropy plays an important role in explaining the working of MSM materials. In the

absence of the external magnetic field, magnetization vectors lie along directions of easy magnetisation. Magnetisation is aligned parallel to one side of the unit cell in each variant.

When an external magnetic field is applied, the magnetisation vector tends to turn from easy direction of the unit cell to the direction of the external magnetic field. If the anisotropy energy is high, the magnetic field strengths required to turn magnetisation off from the easy direction are also high. If the energy of the motion of twin boundaries is low enough compared to the magneto-crystalline anisotropy energy, the external field turns the twin variants, and the magnetisation remains in the original easy direction of the turned unit cells.

As the result, twins in favourable orientation to the magnetic field grow at the expense of the other twins. Ultimately, only one twin variant remain. The reorientation of the twin structure results in the shape change of the material. It is also possible to produce complex shape changes because the reorientation of the twin structures occurs in three dimensions. The original dimensions may be restored by eliminating the field or by turning the field in another direction. Moreover, when a magnetic field is rotated around an MSM element, strain has two maximums on a full circle of 360°. The maximums take place in the field directions perpendicular to the direction in which strain is measured. Stronger magnetic field leads to higher strain. [14].

Measured magnetic-induced-strains of the MSM material can reach 10 % (with fast response times (less than 1 ms). This is significantly more than in any other fast responding actuator material. The reversible magnetic-field-induced strain of MSM material is important in applications. Therefore, the material is often pre-stressed by springs or in other way [13]. A typical characteristic of magnetic field induced strain versus magnetic field in MSM material is reported in the Fig. 3 of ref. [13]. It's worth to note that MSM materials have threshold value around hundreds of kA/m.

### 2.3 Bonding of FBG and MSM

Some efforts have been spent on the integration techniques between active material and FBG. Several gluing techniques have been considered with respect to their ability to transfer the forces between active material and sensor. At this moment cyanoacrilate glue has been tested as the best choice even if during tests its fast aging with temperature increasing has been observed. As a future work some efforts will be spent on the definition of an adequate integration technique.

## 3. Experimentals

### 3.1 Experimental Set-up

#### 3.1.1 Description of the sample

Reported tests have been performed on a sample of 3x5x20 mm<sup>3</sup> Ni-Mn-Ga alloy stick in martensitic state. The crystal structure of the martensitic element is

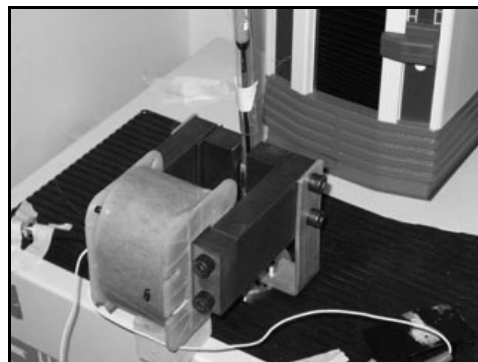


Fig.2 The sample

tetragonal with  $c/a=0.94$ . and  $T_c=95^\circ\text{C}$  and  $T_M=36^\circ\text{C}$ . The characteristic of magnetic field induced strain versus magnetic field for the used sample is similar to the one in Fig. 3 of ref. [13] but with a threshold field value shifted around 250 kA/m and a saturation value of 500 kA/m.

After a suitable bonding protocol choice, followed to improve sensor performances, a fiber Bragg grating (FBG), with a central wavelength,  $\lambda_B$ , free at 1550.14 nm, a 0.890 nm FWHM bandwidth, has been bonded with cyanoacrilate glue on the MSM sample oriented along the principal axis of the MSM element.

The reversibility of magnetic-field-induced strain of MSM material is a very important property in applications. In order to obtain it, the material was pre-stressed. So, the sample was placed in a tension-compression testing system between two aluminium rods.

The compressive stress was applied along the [100] crystallographic direction while the magnetic field was successively applied perpendicular to the stress using an electromagnet opportunely fed.

Magnetization was measured in the direction of the applied magnetic field using a gaussmeter while the strain was measured by using the broadband system based on passive optical filter.

#### 3.1.2 Optoelectronic set-up

The optoelectronic setup used for the proposed magnetic sensor relies on:

- the interrogation optic sensor system previously described, with an optic filter, realized with a chirped and strongly apodized FBG, with a nominal linearity range of 10nm, centered at 1550nm.

- a super luminescent diode with 40nm FWHM bandwidth centered at 1550nm

- a FBG , 0.852nm FWHM bandwidth @  $\lambda_B=1550.14\text{nm}$ .

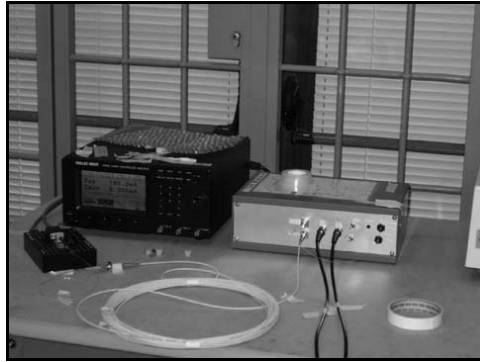


Fig. 3 Optoelectronic set-up

### 3.1.3 Magnetic set up

The magnetic field was applied to the sample through a custom electromagnet. The air gap dimensions are 8x50x20 mm. With this custom configuration we can achieve only a maximum magnetic field value around the threshold value for the MSM material exploited in the air gap using a maximum current of alimention of 2A. In order to fed the electromagnet a Kepco's bipolar BOP power supplies (BOP) has been used. The output range for BOP 100-4M is  $\pm 100V$  for  $E_0$  max and  $\pm 4A$  for  $I_0$  max. Magnetization was measured in the direction of the applied magnetic field using a digital signal processor (DSP) based Hall effect gaussmeter, the Lakeshore 475 DSP. Field ranges for this gaussmeter are from 35 mG to 350 kG while the DC measurement resolution is to 0.02 mG.

### 3.1.4 Mechanical set up

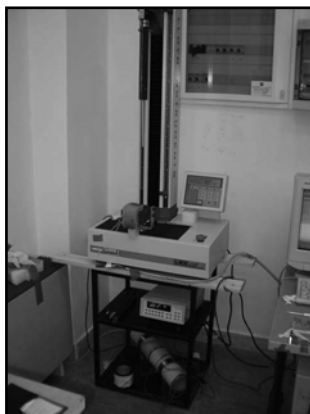


Fig. 4 Mechanical set up

In order to obtain the reversibility of magnetic field induced strain, the sample was pre-stressed using a tension- compression testing system , the Lloyd Instruments LRXPlus 5 kN for material testing applications up to 5 kN (Fig 4)

## 3.2 Experimentals

In order to characterize the sensing system and the material several tests have been performed. To obtain

the reversibility of the magnetic field induced strain the material needs a level of pre-stress. Tests with different pre-stress levels have been performed and for each one, a sinusoidal magnetic field with amplitude up around the threshold value for MSM sample and a frequency of 0.03 Hz has been applied to the structure. Related Gaussmeter and FBG responses have been acquired using a Data Acquisition (DAQ) system Superlogics USB 9803 EC (16-Bit, 100kHz A/D with mass termination connector).

## 4. Results

### 4.1 Magnetic field sensor and sensitivity

For a level of pre-stress on the structure of 15 N in Figs. 5 and 6 are reported:

- the time history of the gaussmeter (Fig. 5)
- the time history of Bragg normalized output signal (Fig.6)

Even though the FBG is initially in a compressive state (due to the 15N pre-stress), this state has been chosed as baseline. Indeed, the curve in Fig. 6 starts from the point  $\Delta V_N=0$ ,  $H=0$  and the first path represents the first magnetization curve for the material.

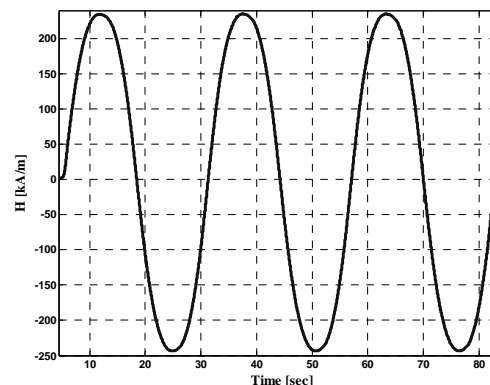


Fig. 5 Gaussmeter signal

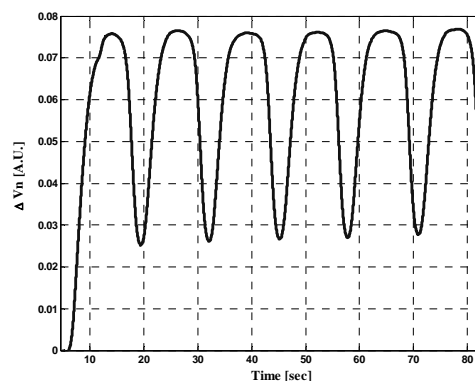
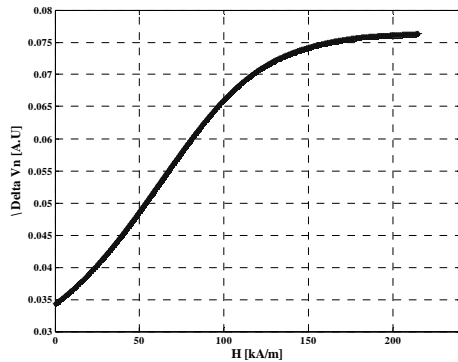


Fig. 6 Bragg normalized signal

In Fig. 7 the sensor characteristic has been reported:



**Fig. 7** Magnetic sensor characteristic

These results confirm the potentialities of FBG as magnetic field sensor. In particular, with the experimental setup above described, the obtained sensitivity, expressed as  $\Delta V_n/(\Delta H/H_m)$ , results of  $2.81e-2$  for applied fields smaller than 100 kA/m and for a level of pre-stress of 15N. The minimum  $\Delta H/H_m$  detectable, under these conditions, is  $7.11e-3$ , where  $H_m$  is the mean magnetic field in the considered range.

#### 4.2 Material characterization

Furthermore, the same setup has been used for MSM material characterization. In Fig. 8 the MSM strain-field characteristic is shown:

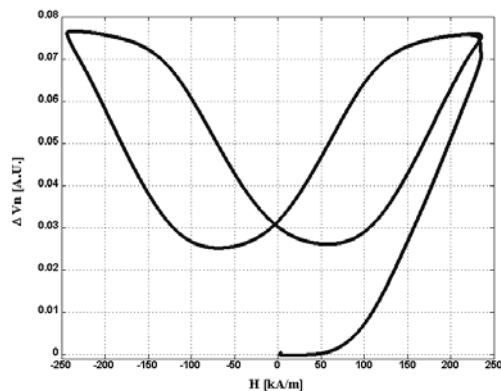


**Fig. 8** Strain field characteristic

The curve starts from the point ( $\Delta V_n=0$ ,  $H=0$ ) and then follows the typical butterfly closed-loop shape. It is worth noting that the first path is outside of the closed-loop because the latter is a minor-loop of the limit-cycle, unreachable with the present setup. As a future work, the development of new set-up able to achieve magnetic field up to 500kA/m is planned. In this way all potentialities of these new material will be overworked.

### 5. Comparison with Terfenol based sensor-

Using the same interrogation sensor system exploited for MSM characterization, tests have been carried out bonding a FBG on a Terfenol sample. Also Terfenol needs a level of pre-stress and in order to excite material a solenoid has been used. Terfenol needs lower magnetic field achieving a non linear range of response already around few tens of kA/m. Several tests have

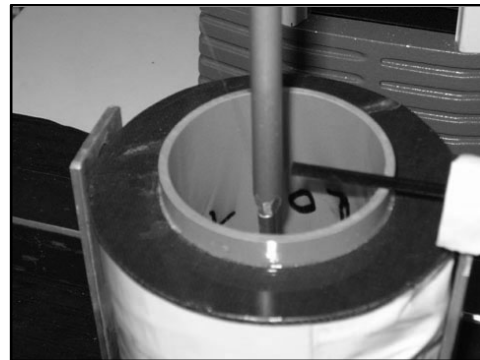


**Fig. 9** Particular of the set up for Terfenol test

been performed with different level of pre-stress. The maximum for magnetic field generated by solenoid is nearly 12 kA/m. For this range of field and for a level of pre-stress of 43N, the sensitivity, expressed as  $\Delta V_n/(\Delta H/H_m)$ , results of  $6.4e-3$  where  $H_m$  is the mean magnetic field in this considered range Whereas the minimum relative resolution,  $\Delta H/H_m$ , detectable with this set up is 0.0312. These results are comparable with those proposed recently in literature [10].

Comparing the characteristics of MSM and Terfenol based sensors, we notice that the linear magnetic field range of MSM is different from Terfenol one, in particular is one order of magnitude higher than Terfenol and this difference holds true also for the threshold values. Therefore, only a relative comparison is possible. So, after a proper calibration procedure carried out in order to obtain the FBG response expressed directly as  $\lambda$ , the relative sensitivity for MSM and Terfenol can be found.

The sensitivity, expressed as  $(\Delta \lambda_B/\lambda_B)/(\Delta H/H_m)$  for MSM results of  $1.6e-4$  while for Terfenol is  $5.1e-5$ .

### 6. Conclusion

The exploitation of FBG as magnetic field sensor has been demonstrated. The FBG has been bonded to the pre-stressed MSM sample. The interrogation optoelectronic system used for the proposed magnetic sensor relies on a low cost ratiometric technique based on optical filtering combined with broadband interrogation. With this set up, the MSM sensitivity, expressed as  $\Delta V_n/(\Delta H/H_m)$ , of  $2.81e-2$  has been achieved. In this work MSM material has not been exploited up its real possibilities. In fact it has been used around its threshold value. In spite of it from all

the preliminary results, it appears that for magnetic field values lower than 30 kA/m, MSM and Terfenol have similar performances. But for all those applications in which higher magnetic field and current are involved MSM results the better choice. In order to further increase the MSM sensitivity and exploit all the linear range, a development of magnetic set up with magnetic field up to 500kA/m has been planned. Furthermore, the analysis of these materials in different working condition and the application of suitable techniques [15] for the compensation of nonlinearities will be carried out in order to increase the sensor's linearity ranges. Also mechanical setup with low pre-stress levels and a better bonding technique will be analysed.

## References

- [1] J. E. Lenz, "A Review of Magnetic Sensors", *Proceedings of the IEEE*, Vol 78, No 6, p. 973 - 989, 1990.
- [2] T. Bosselmann, "Innovative applications of fibre-optic sensors in energy and transportation", *17<sup>th</sup> International Conference on Optical Fibre Sensors, Proceedings of SPIE* Vol. 5855 pp 188-193, 2005
- [3] K. Bohnert, P. Gabus, H. Brändle, P. Guggenbach, "Fiber-optic dc current sensor for the electro-winning industry", *17<sup>th</sup> International Conference on Optical Fibre Sensors, Proceedings of SPIE* Vol. 5855 pp 210-213, 2205
- [4] Tingyu Wang, Chengmu Luo, and Shengxuan Zhen, "A Fiber-Optic Current Sensor Based on a Differentiating Sagnac Interferometer", *IEEE Transactions on Instrumentation and Measurement*, vol. 50, no. 3, June 2001.
- [5] R. M. Measures, "Fibre Optic Sensor Consideration and Developments for Smart Structures" *SPIE* Vol. 1588, "Fiber Optic Smart Structures and Skins IV", pp. 76-85, (1991).
- [6] E. Udd, "Fiber Optic Smart Structures", John Wiley and Sons, New York, (1995).
- [7] D. Inaudi, "Fiber Optic Smart Sensing", in: *Optical Measurements Techniques and Applications*, (P.K. Rastogi ed.), Artech House, Boston, pp. 255-274, (1997).
- [8] B. Culshaw and J. Dakin, "Optical Fiber Sensors: Applications, analysis, and future Trends", Artech House inc., Norwood, (1997).
- [9] A. Cusano, A. Cutolo, G. Breglio, M. Giordano, L., Nicolais, "Low Cost All-Fiber Bragg Grating Sensing System for Temperature and Strain Measurements", *Optical Engineering*, Vol.5706, 1-10, 2005.
- [10] J. Mora, A. Díez, J. L. Cruz, and M. V. Andrés, "A Magnetostrictive Sensor Interrogated by Fiber Gratings for DC-Current and Temperature Discrimination", *IEEE Photonics Technology Letters*, Vol. 12, No. 12, pp. 1680 - 1682, 2000.
- [11] Cusano A., Breglio G., Giordano M., Nicolais L., Cutolo A., "A Multifunction fiber optic sensing system for smart applications", *IEEE/ASME Transactions on Mechatronics*, 9(1), 40-50, 2004.
- [12] Caponero M.A., Felli F., Paolozzi A., "Strain Measurements with FBGs Embedded into Cast Metal Alloys", *7th Japan Int. SAMPE Symp. and Exhibition (JISSE 7)*, pp. 661-664, Tokyo, Nov. 2001.
- [13] J. Tellinen, I. Suorsa, A. Jääskeläinen, I. Aaltio and K. Ullakko "Basic Properties of Magnetic Shape Memory Actuators", *8th international conference ACTUATOR 2002*, Bremen, Germany, 10-12 June 2002.
- [14] T. Jokinen, K. Ullakko, I. Suorsa, "Magnetic Shape Memory Materials-New possibilities to create force and movement by magnetic fields", *Electrical Machines and Systems*, [20-23], 2001 ICEMS (2001).
- [15] C. Natale, F. Velardi, C. Visone, "Modelling and Compensation of Hysteresis for Magnetostrictive Actuators", *IEEE/ASME Int. Conf. on Advanced Intelligent Mechatronics*, Como, I, 2001